Assessment Of In Silico Antioxidant, Anti-Inflammatory, And Antidiabetic Activites Of Ximenia Americana L. Olacaceae

Mubarak Muhammad Dahiru[1*], Mahmud Bala Alfa[2],
Maimuna Abdulrahman Abubakar[3], Aliyu Pela Abdullahi[4]

[1]Adamawa State Polytechnic, Yola, School of Science and Technology, Pharmaceutical Technology Department, 640101, Yola, Nigeria.
[2,3&4]Modibbo Adama University, Faculty of Life Sciences, Biochemistry Department, 640261, Yola, Nigeria.

Emails: mubaraq93@adamawapoly.edu.ng, mahmudbalaalfa@mau.edu.ng, maimunaabdulrahmanabubakar@mau.edu.ng, Aliyupela@mau.edu.ng

Abstract:

Persistent hyperglycemia leading to oxidative stress and inflammatory response contributes to the pathology of diabetes. This study investigated the antioxidant, anti-inflammatory, and antidiabetic potential of Ximenia americana (XA) L. Olacaceae in silico exploring its possible mechanism of action. The study was carried out by molecular docking of the compounds present in XA with the antioxidant, anti-inflammatory, and antidiabetic targets followed by molecular dynamics simulation. Stigmasterol exhibited the lowest respective binding affinity and inhibition constant with xanthine oxidases (-8.7 kcal/mol and 4.13 ×10-1 μM), cytochrome p450 21A2 (-11.5 kcal/mol and 3.64 × 10-3 μM), myeloperoxidase (-10 kcal/mol and 4.59 × 10-2 μM), phospholipase A2 (-9.3 kcal/mol and 1.50 × 10-1 μM), inducible nitric oxide synthase (-10.8 kcal/mol and 1.19 × 10-2 μM), 11β hydroxy-steroid dehydrogenase 1 (-9.4 kcal/mol and 1.27×10-1 μM), and alpha-amylase (-9.6 kcal/mol and 1.27×10-1 μM), while 4,4-Dimethylcyclohex-2-en-1-ol showed the least BA (-7.6 kcal/mol) and Ki (2.65 μM) with interleukin associated kinase 4. Furthermore, the molecular dynamics simulation shows high residue displacements of up to 6.11, 3.69, 4.97, 5.24, 4.21, 4.41, 5.80, and 5.76 Å for xanthine oxidase, cytochrome p450 21A2, myeloperoxidase, phospholipase A2, inducible nitric oxide synthase, interleukin associated kinase 4, alpha-amylase, and 11β hydroxy-steroid dehydrogenase 1, respectively. Conclusively, stigmasterol and 4,4-Dimethylcyclohex-2-en-1-ol might be the key compounds involved in the antioxidant, anti-inflammatory, and antidiabetic activity of XA via inhibition of the enzymes involved in oxidative stress, inflammation, and diabetes.
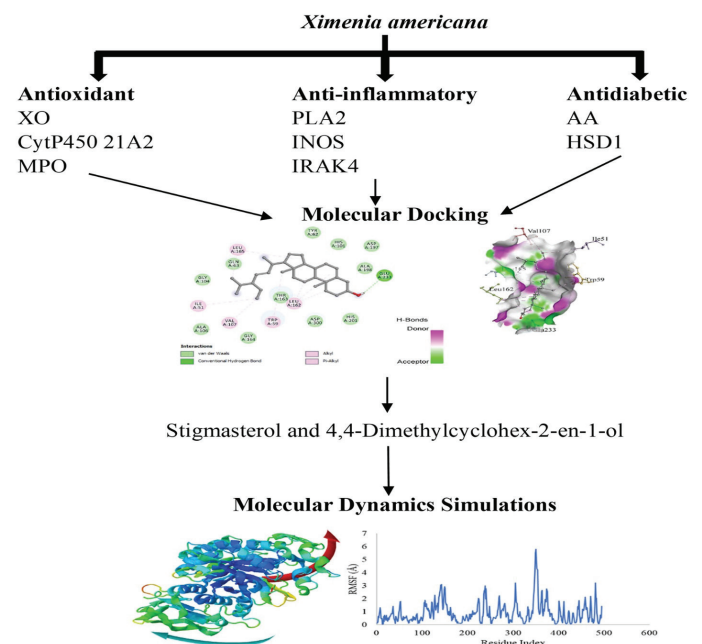
1. Introduction

Oxidative stress (OS) and inflammation have been regarded as key contributors to the pathophysiology of diabetes induced by its associated persistent and recurrent hyperglycemia (Yousef et al., 2023). Diabetes is evolving and as more knowledge is coming to light, it is regarded as an inflammatory-mediated condition caused by increased reactive oxygen species (ROS)

generation originating from hyperglycemia (Korac et al., 2021; Oguntibeju, 2019). Persistent hyperglycemia promotes the generation and accumulation of ROS along with the activation of pathways including hexosamine, polyol, protein kinase C, and the formation of advanced glycation end products (AGEs) leading to mitochondrial dysfunction and cellular damage (Sangwung et al., 2020). The ROS generation creates a redox imbalance in the cell due to depletion of the inherent antioxidant system, thus, activating redox responses including the transcription and expression of redox proteins and subsequent manifestation of low-grade inflammation (Wronka et al., 2022). The persistent redox imbalance activates proinflammatory proteins and the subsequent release of inflammatory cytokines by infiltrating macrophages (Zhang et al., 2020). This occurs predominantly in the visceral white adipose tissues. The ROS generation coupled with the low-grade inflammation from hyperglycemia contributes to the development of diabetes *via* insulin resistance by obstructing insulin signaling (Oguntibeju, 2019).

In diabetes, the endoplasmic reticulum, phagocytic cells, and peroxisomes are the sites for ROS generation influenced by the mitochondrial electron transport chain with the ROS accumulation leading to intracellular disturbance in the insulin signaling pathway and promoting its resistance (Bhatti et al., 2022). Although ROS generations are beneficial in some instances, their accumulation is harmful to the cells as observed in diabetes (Shields et al., 2021). Moreover, hyperglycemia promotes hypoxia and macrophage invasion releasing cytokines and chemokines further promoting inflammatory responses leading to insulin resistance and diabetes (Ellulu & Samouda, 2022). Thus, OS and inflammation promoted by persistent hyperglycemia are regarded as major culprits in the development of insulin resistance in diabetes. Different treatments are employed to manage oxidative stress and inflammatory conditions in diabetes including antidiabetic drugs to minimize their damage (Dahiru, 2023; Dahiru & Nadro, 2022; Wronka et al., 2022). However, the adverse effects and cost of these drugs lead to consideration for alternatives such as plant-based therapies and other natural products. Furthermore, different proteins were previously reported as antidiabetic targets *via* molecular docking and molecular dynamics simulations (Dahiru et al., 2023). Additionally, several plants exert antidiabetic (Przeor, 2022), anti-inflammatory (Gandhi et al., 2022), and antioxidant (Nwozo et al., 2023) properties attributed to their phytoconstituents (Dahiru, 2023) including *Ximenia americana* (XA) (Bakrim et al., 2022; Shettar et al., 2015; Shettar et al., 2017).

XA has various nutritional and pharmacological applications formulated in different preparations (Kefelegn & Desta, 2021). The high concentration of monounsaturated and saturated fatty acids content of the plant contributes to its resistance to oxidation (Kefelegn & Desta, 2021). XA was shown to attenuate chronic inflammation *via* suppressing or regulating inflammatory mediators (da Silva et al., 2023). Moreover, heteropolysaccharides from XA interacted with the cannabinoid receptor 2 inhibiting inflammation (da Silva-Leite et al., 2018). The antidiabetic activity of the plant was attributed to its hypoglycemic effects (Shettar et al., 2017). In our study, *in silico* investigations were carried out on the antioxidant, anti-inflammatory, and antidiabetic potential of XA to evaluate its possible mechanism of action by molecular docking and molecular dynamic simulation.

2. Materials and Methods

1.1 Materials
1.1.1 Hardware specification

The present study utilized a personal computer (HP Envy M6 K010dx) with an 8 GB RAM and AMD 2.1 GHz to 2.9 GHz Elite Quad-core A10-5745M accelerated processer and AMD Radeon HD 8610G graphics with up to 3053 MB total graphics memory.

1.1.2 Ligands and targets

The ligands (compounds) used in the present study were previously reported in our study (Dahiru et al., 2022). The standard drugs, including allopurinol (PubChem ID; 135401907), aspirin (PubChem ID;2244), and metformin (PubChem ID; 4091) were used as antioxidant, anti-inflammatory, and antidiabetic standard drugs, respectively. The 3D structures of the compounds and standards were downloaded in SDF format from the PubChem database (https://pubchem.ncbi.nlm.nih.gov). The PubChem IDs of the compounds are shown in Table 1. Furthermore, the ligands and standards were energy-minimized using the PyRx software (version 0.8) before docking. The docking targets were downloaded from the RSCB protein data bank (https://www.rcsb.org) in PDB format and prepared by removing heteroatoms, water molecules, and multiple chains using the AutoDockTools software (version 1.5.7) (Sanner, 1999) and saved in PDB format. These docking targets were previously reported to be associated with the pathology of oxidative stress, inflammation, and diabetes.

Table 1. List of Ligands

Name	PubChem ID
Catechol	289
Phloroglucinol	359
Hydroquinone	785
Palmitic acid	985
Pyrogallol	1057
Methyl palmitate	8181
5-Methyl-1H-pyrazole-3-carboxylic acid	9822
Hydroxyquinol	10787
Tridecane	12388
Pentadecanoic acid	13849
2-Isopropoxyphenol	20949
2-dodecoxyethanol	24750
5-Acetoxymethyl-2-furaldehyde	66349
6-Methylpyridazin-3(2H)-one	83346
3,4-dimethylcyclohexanol	97960
2,6-Heptanedione	100532
5-Butylnonane	300476
Oleic acid	445639
3,8-Dimethyldecane	519396
Tetradec-13-enal	522841
Stigmasterol	5280794
1-(1-Butenyl) pyrrolidine	5357122
7,11-Hexadecadien-1-ol, acetate, (7Z,11Z)-	5363265
9-Tetradecenal, (Z)-	5364471
4,4-Dimethylcyclohex-2-en-1-ol	19771306

The docking targets are shown in Table 2 including the docking coordinates identified by the Prank Web Ligand Binding Site Prediction online server (https://prankweb.cz) (Jendele et al., 2019).

Table 2. List of Target

Targets		RSCB ID X	Docking coordinates	
			Y	Z
Antioxidant	Xanthine oxidase (XO)	3NVZ	23.12	-16.04	35.78
	Cytochrome P450 21A2 (CytP450 21A2)	4Y8W	-14.66	12.03	28.61
	Myeloperoxidase (MPO)	7LAL	19.13	-13.61	-4.49
Anti-inflammatory	Phospholipase A2 (PLA2)	1KVO	-38.77	63.21	32.38
	Inducible nitric oxide synthase (INOS)	4NOS	0.57	97.02	19.69
	Interleukin-1 receptor-associated kinase 4 (IRAK4)	5KX7	28.49	39.24	10.57
Antidiabetic	11-beta-hydroxysteroid dehydrogenase (HSD1)	3D3E	5.65	0.23	13.14
	Alpha amylase (AA)	3BAJ	10.04	17.16	45.59

1.2 Methods
1.2.1 Molecular Docking (MD)
The PyRx software vina wizard was utilized for the MD by setting the exhaustiveness to 16 to determine the binding affinity (BA) followed by the visualization of the docking interactions using the Biovia Discovery Studio Visualizer software (version 16.1.0). The equation $K_i = \exp \Delta G/RT$ was used to determine the inhibition constant (K_i) where ΔG, R, and T signify binding affinity, universal gas constant (1.985×10^{-3} kcal^{-1} mol^{-1} k^{-1}), and Temperature (298.15 K), respectively (Ortiz et al., 2019). The top-docked compounds with the best docking interactions were selected.

1.2.2 Molecular Dynamics Simulation (MDS)

The iMODs server (https://imods.iqfr.csic.es) (iMODS) (López-Blanco et al., 2014) and CABs flex v2.0 (http://biocomp.chem.uw.edu.pl/CABSflex2/index) (Kurcinski et al., 2019) online servers were used for the MDS to identify cluster motion and residue displacements of the top docked complexes, respectively.

3.   Results and Discussion

In the present study, the antioxidant, anti-inflammatory, and antidiabetic potential of XA was explored by molecular docking and dynamics. This was aimed at predicting its possible mechanism of action from the interactions of the compounds identified from the plant with the proteins involved in oxidative stress, inflammation, and diabetes. Hyperglycemia, oxidative stress, and inflammation are key contributors to the pathology of diabetes. Thus, attenuation of these processes will be vital in the management of the ailment.

Table 3 displays the BA and Ki of the binding interactions of XO with the compounds and allopurinol. The lowest BA (-8.7 kcal/mol) and Ki (4.13 ×10^{-1} µM) were exhibited by stigmasterol next to 4,4-Dimethylcyclohex-2-en-1-ol with BA and Ki of -7.7 kcal/mol and 2.24 µM, respectively. Allopurinol exhibited the highest BA (-5.9 kcal/mol) and Ki (46.82 µM) compared to the top three docked compounds. Figure 1 exhibits the respective 3D and 2D docking interactions of XO with stigmasterol (a and d) and allopurinol (b and e) revealing the interactions including the participating residues. Stigmasterol exhibited two alkyl and a pi-Sigma interactions while allopurinol demonstrated 6 hydrogen bonds (HB).

The BA and Ki of the docking interaction of Cytp450 21A2

with the compounds and allopurinol are presented in Table 3. The lowest BA (-11.5 kcal/mol) and Ki (3.64 × 10^{-3}µM) were demonstrated by stigmasterol followed by 4,4-Dimethylcyclohex-2-en-1-ol with BA and Ki of -8.6 kcal/mol and 4.89× 10^{-1} µM, respectively. The highest BA (-6.4 kcal/mol) and Ki (20.12 µM) were exhibited by allopurinol compared to the top three compounds. Furthermore, the respective 3D and 2D interactions of CytP450 21A2 with stigmasterol (c and f) and allopurinol (g and j) with Cytp450 21A2 are depicted in Figure 1. The docking interaction reveals the formations of an HB and 10 alkyl interactions by stigmasterol while allopurinol exhibited 3 HBs only.

The BA and Ki originating from the docking interactions of MPO with the compounds are displayed in Table 3. Stigmasterol had the lowest BA (-10 kcal/mol) and Ki (4.59 × 10^{-2} µM) followed by 4,4-Dimethylcyclohex-2-en-1-ol with BA and Ki of -7.3 kcal/mol and 4.40 µM, respectively. Additionally, allopurinol exhibited the highest BA (-6.4 kcal/mol) and Ki (20.12 µM) compared to the top two docked compounds. Furthermore, the respective 3D and 2D dock pose and interactions are shown in Figure 1 revealing the binding interactions of MPO with stigmasterol (h and k) and allopurinol (i and l). A maximum of 10 alkyl interactions were exhibited by stigmasterol involving different residues while allopurinol exhibited 3 HBs.

Table 3. Binding Interaction of XO, CytP450 21A2, and MP with the Compounds and Aspirin

Target	Ligand	Binding Affinity (kcal/mol)	Inhibition Constant (µM)
XO	Stigmasterol	-8.7	4.13 ×10^{-1}
	4,4-Dimethylcyclohex-2-en-1-ol	-7.7	2.24
	Pyrogallol	-6.7	12.12
	Allopurinol	-5.9	46.82
CytP450 21A2	Stigmasterol	-11.5	3.64 × 10^{-3}
	4,4-Dimethylcyclohex-2-en-1-ol	-8.6	4.89× 10^{-1}
	Oleic Acid	-6.5	17
	Allopurinol	-6.4	20.12
MPO	Stigmasterol	-10	4.59 × 10^{-2}
	4,4-Dimethylcyclohex-2-en-1-ol	-7.3	4.4
	Allopurinol	-6.4	20.12
	5-Acetoxymethyl-2-furaldehyde	-5.9	46.82

Figure 1 shows the 3D and 2D docking interaction of stigmasterol and allopurinol with XO, Cytp450, and MPO depicting the dock poses.
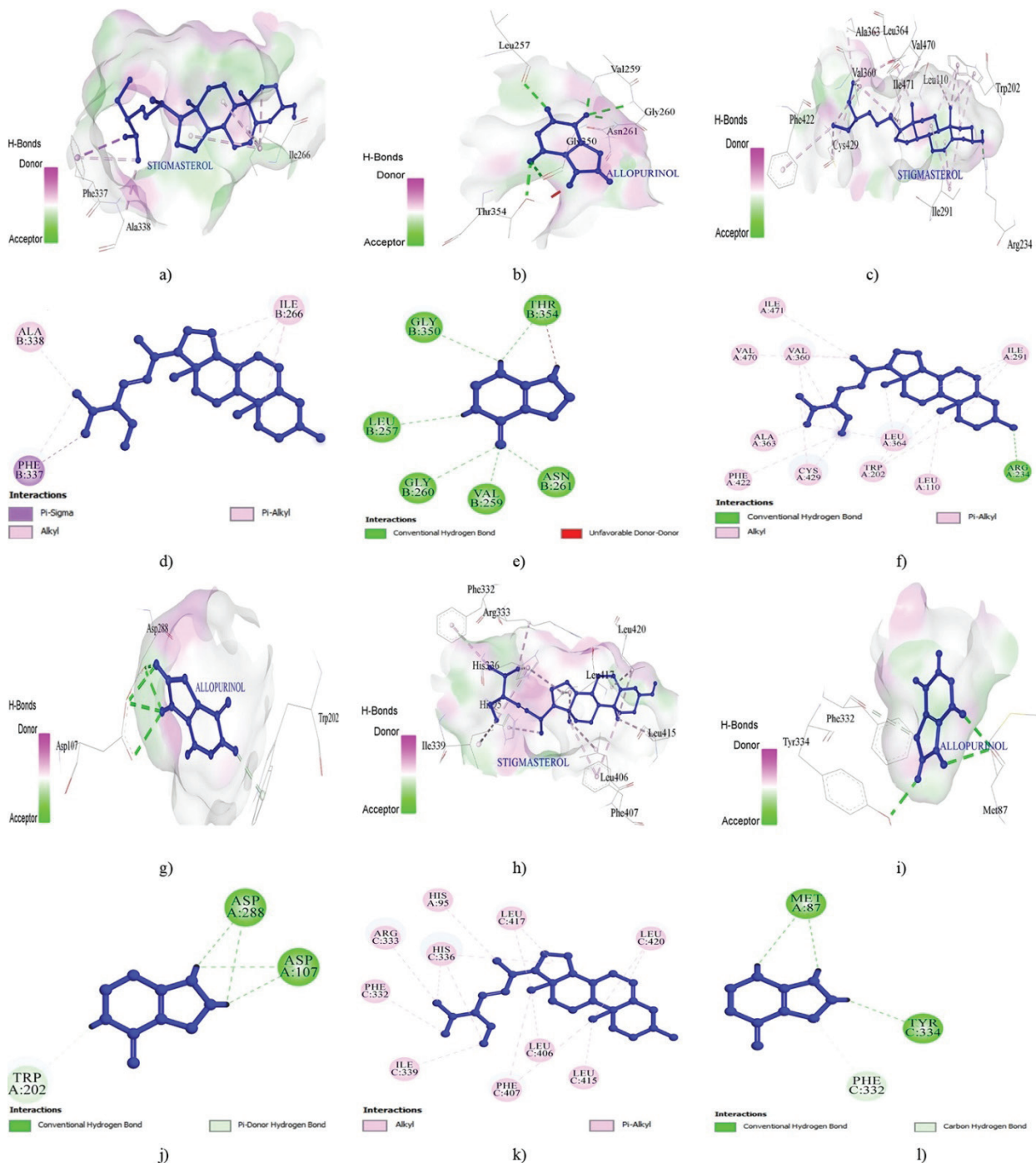
Figure 1. The respective 3D and 2D dock pose of stigmasterol and allopurinol with XO; stigmasterol (a and d) and allopurinol (b and e), Cytp450 21A2; stigmasterol (c and f) and allopurinol (g and j), MPO; stigmasterol (h and k) and allopurinol (i and l)

The MDS result of XO docked with stigmasterol and allopurinol is depicted in Figure 2 showing cluster (a) and residue (b) movements. The overall cluster opposing movement was observed at both sides of the structure. Furthermore, the MDS shows a lot of residue fluctuation within the target structure with notable higher displacements (6.08 and 6.11 Å, respectively) observed at the N-terminal (Thr2) for stigmasterol only and C-terminal (Cys1325) ends of the protein chain for both stigmasterol and allopurinol. XO is involved in purine metabolism catalyzing the breakdown of xanthine to hypoxanthine then uric acid and generating ROS including superoxide and peroxide in the process. Thus, a target for minimizing OS by lowering its activity (Singh et al., 2023). In our study, stigmasterol exhibited a favorable interaction with XO with a low BA and Ki suggesting a possible activity disruption. Additionally, the MDS showed a lot of displacement within the peptide structure suggesting many hinge regions and possible deformability of the peptide. Although stigmasterol

demonstrated lower BA and Ki compared to allopurinol, the latter exhibited a higher number of HBs which might translate to a more stable and stronger complex (Ferenczy & Kellermayer, 2022), a typical property of standard drugs.

The MDS result of CytP450 21A2 docked with stigmasterol and allopurinol depicting cluster movement (c) and residue fluctuation (d) is presented in Figure 2. A high cluster movement was observed at the carboxyl end of the peptide while the amino terminal moved in the opposite direction. Notable residue fluctuations were observed at both ends though higher at the tail end. Moreover, major fluctuations were observed for stigmasterol at Leu38 (3.45 Å), Ile132 (2.90 Å), Pro155 (3.28 Å), and Gln276 (3.31 Å) with the highest seen at Ser333 (3.69 Å). However, higher fluctuations were observed for allopurinol at Ala251 (3.07 Å), Val414 (3.48 Å), Val428 (2.53 Å), Gly456 (4.07 Å), and Gly485 (3.06 Å). The cytp450 enzyme families are expressed throughout the body and are vital for several physiological functions. However, their activities are coupled with ROS generation (Veith & Moorthy, 2018). CytP450 21A2 catalyzes the vital step in adrenal steroid synthesis *via* progesterone and 17α-hydroxyprogesterone hydroxylation (Pallan et al., 2015). However, it generates carbon radicals (Yoshimoto et al., 2012), thus, a target to minimize OS. In the researchers' report, the low BA and Ki observed in the interaction of stigmasterol with CytP450 21A2 might inhibit the enzyme activity *via* tertiary structure disruption as the MDS result showed several residue displacements indicating hinge regions within the peptide. Moreover, allopurinol showed higher HBs which might contribute to stronger interaction compared to stigmasterol.

Figure 2 depicts the MDS result of MPO docked with stigmasterol and allopurinol showing cluster (e) and residue (f) fluctuations. Higher cluster fluctuations for stigmasterol were observed at Gly23 (3.54 Å), Asp39 (3.91 Å), Ser191 (3.81 Å), Glu354 (4.97 Å), Pro445 (2.93 Å), and Arg487 (3.01 Å). However, higher fluctuations were observed for allopurinol at Cys1 (6.26 Å), Asn54 (4.33 Å), Val113 (3.85 Å), Pro132 (4.55 Å), Phe146 (6.88 Å), Ile551 (2.76 Å), and Ser569 (2.74 Å). MPO is an important part of the innate immune system secreted by neutrophils and macrophages with oxidoreductase activity generating microbicidal oxidants from chloride and peroxide yielding HOCl. Thus, generating ROS in the process (Chen et al., 2020). Decreased activity of the enzyme might lead to improvement in oxidative stress-associated ailments. In this report, the low BA and Ki exhibited by stigmasterol might indicate an inhibition of MPO activity, further supported by the MDS result showing different hinge

regions within the enzyme structure. Thus, the binding of stigmasterol to the enzyme might lead to tertiary structure disruption. However, allopurinol demonstrated a possible stronger interaction with a higher number of HBs.
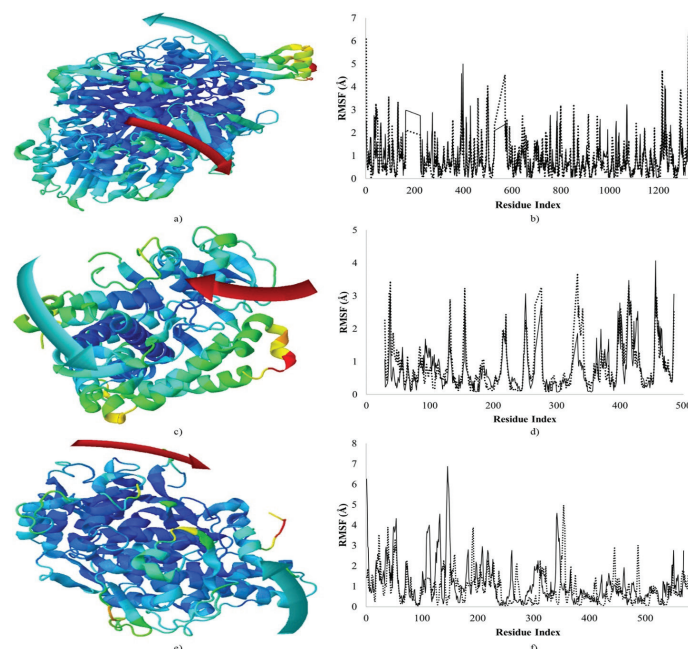

Figure 2. MDS result of stigmasterol and allopurinol showing respective cluster movement and residue fluctuations of the docked complexes; XO (a and b), Cytp450 21A2 (c and d), MPO (e and f)

The docking interactions of PLA2 with the compounds and aspirin revealing the BA and Ki are displayed in Table 4. Stigmasterol exhibited the lowest BA (-9.3 kcal/mol) and Ki (1.50×10^{-1} μM) next to 4,4-Dimethylcyclohex-2-en-1-ol with -7.9 kcal/mol and 1.6 μM, respectively. Aspirin exhibited the highest BA (-5.7 kcal/mol) and Ki (65.65 μM) compared to the top three compounds. Furthermore, the respective 3D and 2D dock poses are presented in Figure 3 depicting the binding interactions of stigmasterol (a and d) and aspirin (b and e) with PLA2. Notable interactions by stigmasterol, include 1 HB (ASP48) and 9 alkyl interactions. Although aspirin had the highest BA and Ki, it demonstrated superior HB (2) interaction compared to stigmasterol.

The docking interactions of INOS with the compounds and aspirin are displayed in Table 4 showing the BA and Ki. The lowest BA (-10.8 kcal/mol) and Ki (1.19×10^{-2} μM) were exhibited by stigmasterol followed by 4,4-Dimethylcyclohex-2-en-1-ol with -8.2 kcal/mol and 9.61×10^{-1} μM, respectively. Aspirin had a higher BA (-6.8 kcal/mol) and Ki (10.23 μM) compared to the top two compounds. Moreover, the dock poses of INOS with stigmasterol (c and f) and aspirin (g and j) are shown in

Figure 3 depicting the respective 3D and 2D interactions. The major interaction for stigmasterol was the alkyl (10) and a pi-sigma with Trp372 while aspirin exhibited 2 HBs in addition to a pi-sigma and alkyl with Phe369 and Leu209.

The docking interaction of IRAK4 with the compounds and aspirin is shown in Table 4 depicting the BA and Ki. 4,4-Dimethylcyclohex-2-en-1-ol exhibited the least BA (−7.6 kcal/mol) and Ki (2.65 μM) followed by stigmasterol

with −7.2 kcal/mol and 5.21 μM, respectively. Aspirin exhibited the highest BA (−6.4 kcal/mol) and Ki (20.12 μM) compared to the top two compounds. Furthermore, the respective 3D and 2D dock pose of the interaction of IRAK4 with 4,4-Dimethylcyclohex-2-en-1-ol (h and k) and aspirin (i and l) is displayed in Figure 3. A total of 2 HBs and 7 pi interactions were observed for stigmasterol including pi sulfur with Met192 while aspirin exhibited an HB (Leu248), alkyl (Leu245), and pi-sigma (Met237).

Table 4. Binding Interaction of PLA2, INOS, and IRAK4 with the Compounds and Aspirin

Target	Ligands	Binding Affinity (kcal/mol)	Inhibition Constant (μM)
PLA2	Stigmasterol	−9.3	1.50×10^{-1}
	4,4-Dimethylcyclohex-2-en-1-ol	−7.9	1.6
	Oleic Acid	−6.1	33.4
	Aspirin	−6	39.55
INOS	Stigmasterol	−10.8	1.19×10^{-2}
	4,4-Dimethylcyclohex-2-en-1-ol	−8.2	9.61×10^{-1}
	Aspirin	−6.8	10.23
	7,11-Hexadecadien-1-ol, acetate, (7Z,11Z)-	−6.7	12.12
IRAK4	4,4-Dimethylcyclohex-2-en-1-ol	−7.6	2.65
	Stigmasterol	−7.2	5.21
	Aspirin	−6.4	20.12
	Oleic Acid	−6	39.54

Figure 3 depicts the dock poses of top-docked compounds and aspirin with PLA2, INOS, and IRAK4 revealing the binding 3D and 2D binding interactions.
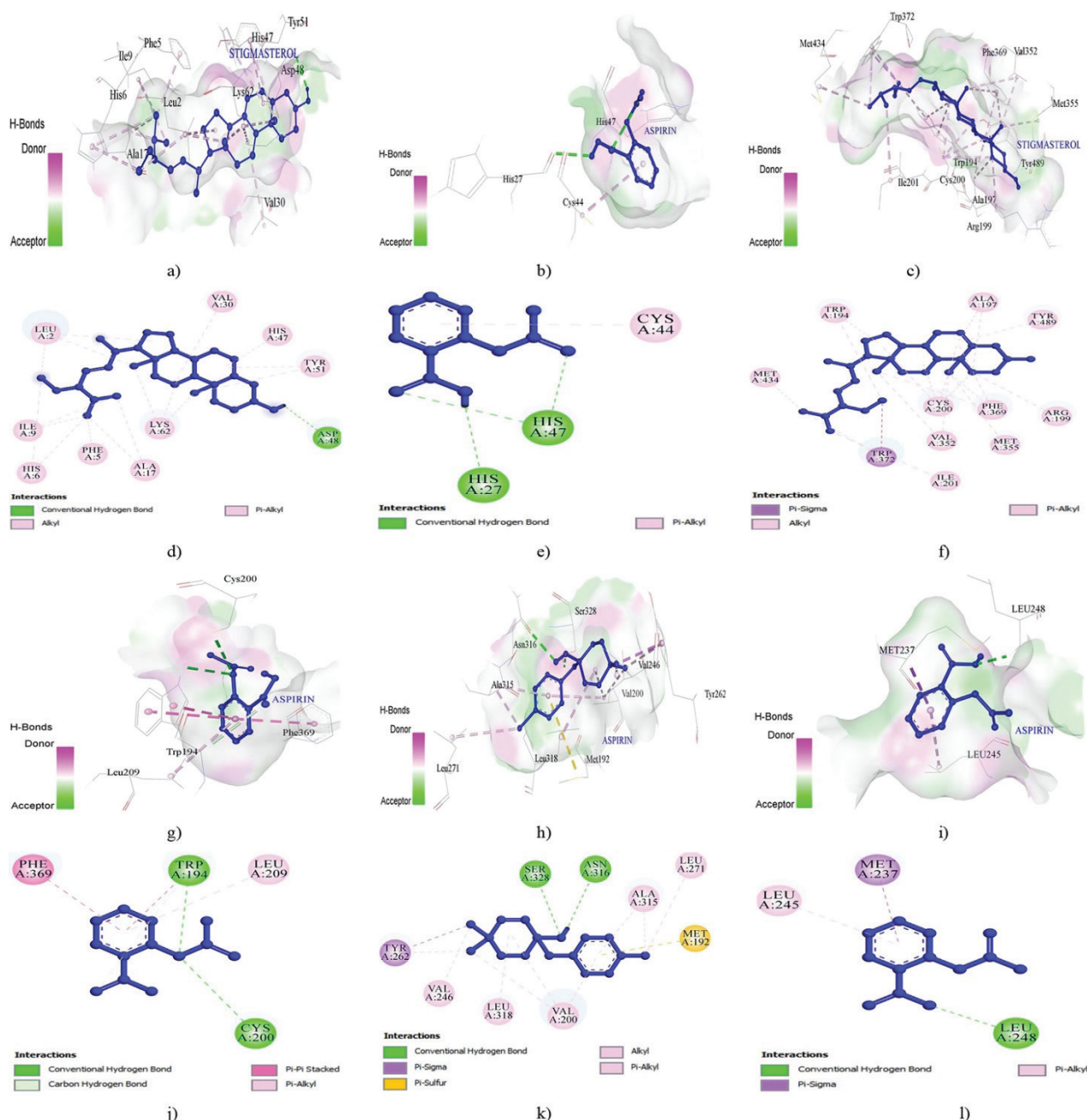
Figure 3. The respective 3D and 2D dock pose of the top docked compounds and aspirin with PLA2; stigmasterol (a and d) and aspirin (b and e), INOS; stigmasterol (c and f) and aspirin (g and j), MPO; 4,4-Dimethylcyclohex-2-en-1-ol (h and k) and aspirin (i and l)

The MDS result of PLA2 docked with stigmasterol and aspirin is presented in Figure 4 depicting the cluster (a) and residue (b) fluctuation. Although there were fluctuations at the N-terminal, the highest residue and cluster fluctuation were observed at the C-terminal for stigmasterol at Lys115 (5.24 Å). Further fluctuations were observed at Gly14 (2.69 Å), Gly29 (2.82 Å), Thr61 (3.46 Å), and Cys124 (3.89 Å), generating a pattern of increasing fluctuation from the N- to C-terminal. For aspirin, the highest fluctuation was at the N-terminal at Asn1 (2.34 Å). Thus, higher fluctuations were observed for the stigmasterol-docked PLA2 complex. The PLA2 enzymes catalyze glycerophospholipids hydrolysis yielding free

fatty acids including arachidonic acid (Chalimoniuk, 2012). Increased concentration of arachidonic acid depletes glutathione promoting the inflammatory process (Chalimoniuk, 2012). Moreover, excess PLA2 activity accumulates free fatty acids and promotes prostaglandin synthesis generating free radicals and proinflammatory cytokines (Chalimoniuk, 2012). Therefore, inhibition of its activity might be beneficial in inflammation-associated ailments like diabetes. In the present study, stigmasterol exhibited a low BA and Ki interaction with PLA2 stabilized by HB and van der Waal interactions possibly inhibiting its activity. Moreover, the MDS result showed the presence of hinge regions

between the helices of the structure indicating possible inhibition induced by ligand binding.

The MDS result of INOS docked with stigmasterol and aspirin is presented in Figure 4 revealing the cluster (c) and residue (d) fluctuations. The highest residue (4.21 Å) and cluster fluctuation for stigmasterol was observed at the N-terminal of the peptide at Ser112 next to residue Lys405 (3.45 Å) at the C-terminal cluster. However, other residue fluctuations were observed for aspirin at Gly93 (2.77 Å), His102 (3.23 Å), and Asn239 (2.63 Å). Fluctuations higher than stigmasterol were observed at Asp274 (4.55 Å), Gly300 (3.06 Å), Gly313 (3.15 Å), Pro323 (2.92 Å), and Gln502 (4.21 Å). Therefore, much higher fluctuations were observed for aspirin. INOS catalyzes nitric oxide synthesis from L-arginine. It is involved in inflammatory response mediation, exacerbating the process *via* its product nitric oxide which regulates and promotes cyclooxygenase-2 synthesis involved in inflammation (Papi et al., 2019). Moreover, an increased level of INOS is observed during inflammation. The present study depicts a low BA and Ki interaction of stigmasterol revealing a possible inhibition of the enzyme and subsequent anti-inflammatory effect of stigmasterol further supported by the observed cluster and residue displacements within the enzyme structure in the MDS.

Figure 4 shows the MDS result of IRAK docked with 4,4-Dimethylcyclohex-2-en-1-ol depicting the cluster (e) and residue (f) fluctuations. Cluster and residue fluctuations for 4,4-Dimethylcyclohex-2-en-1-ol were observed at the N- and C- terminals though the highest (4.41 Å) fluctuation was observed midchain (Glu337) of the peptide. Further fluctuations were observed at Phe323 (2.52 Å), Glu389 (2.02 Å), Lys416 (2.31 Å) and Ala459 (2.91 Å). However, aspirin showed higher fluctuations at Gly195 (2.28 Å), Lys202 (4.32 Å), Gln232 (3.56 Å), Gly255 (3.73 Å), Gly350 (2.66 Å), and Pro445 (2.77 Å). IRAK4 belongs to a family of kinases that modulate inflammatory processes with their absences reported to increase susceptibility to microbial infections. IRAK4 acts as a downstream signal transducer of the interleukin-1 receptor, interleukin-18 receptor, and the Toll-like receptors which are involved in signal receiving, propagation, and amplification (De Nardo et al., 2018). The position of IRAK4 in the signaling cascade prompts its anti-inflammatory target susceptibility (De Nardo et al., 2018). In the present study, 4,4-Dimethylcyclohex-2-en-1-ol exhibited the lowest BA and Ki interaction with IRAK4 possibly inhibiting its activity with the MDS showing residue fluctuations and flexibility.
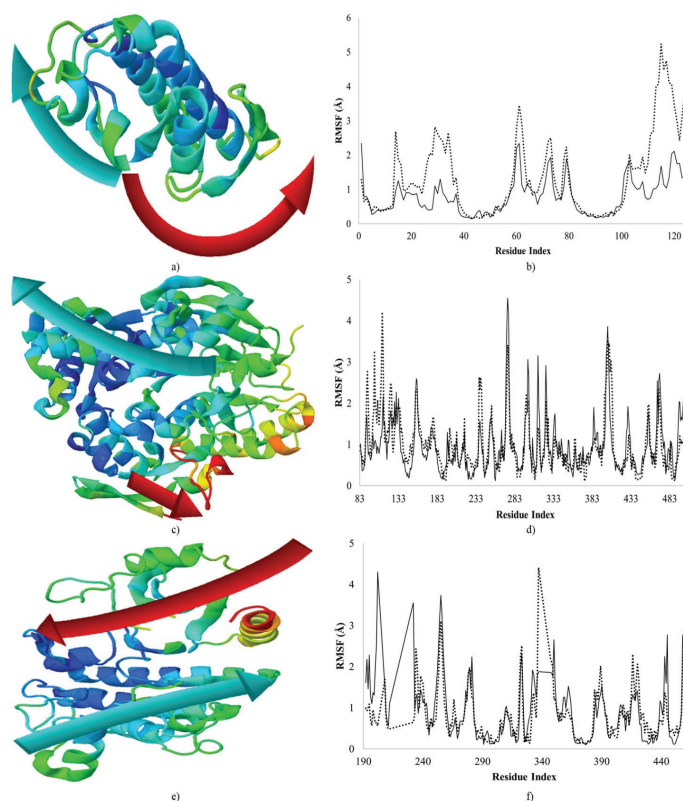

Figure 4. MDS result of the top docked compounds and aspirin showing respective cluster movement and residue fluctuations of the docked complexes; PLA2 (a and b), INOS (c and d), IRAK4 (e and f)

The docking interactions of AA with the compounds and metformin are presented in Table 5 depicting the BA and Ki. Stigmasterol exhibited the lowest BA (-9.6 kcal/mol) and Ki (9.02×10^{-2} μM) next to 4,4-Dimethylcyclohex-2-en-1-o with -7.4 kcal/mol and 3.71 μM, respectively. Metformin demonstrated the highest BA (-5.2 kcal/mol) and Ki (152.81 μM) compared to the top five compounds. Moreover, the respective 3D and 2D dock poses and binding interactions of AA with stigmasterol (a and b) and metformin (c and d) are shown in Figure 5. A HB was formed with Glu233 by stigmasterol in addition to 5 alkyl interactions. For metformin, a HB was observed with His299 in addition to the salt bridge, attractive charge, and pi-cation interactions.

Table 5 exhibits the BA and Ki of the binding interactions of HSD1 with the compounds and metformin. Stigmasterol exhibited the lowest BA (-9.4 kcal/mol) and Ki (0.13 μM) followed by 4, 4-Dimethylcyclohex-2-en-1-ol with BA and Ki of -7.2 kcal/mol and 5.21 μM, respectively. The highest BA (-5.6 kcal/mol) and Ki (77.73 μM) were exhibited by metformin compared to the top five compounds. Furthermore, the respective 3D and 2D interactions of HSD1 with stigmasterol (e and f) and metformin (g and h) are shown in Figure 5 revealing the dock pose and

binding interactions. The major interaction observed for stigmasterol was the HB with Glu233 and 5 alkyl interactions while metformin exhibited 3 HBs in addition to an attractive interaction with Asp132.

Table 5. Binding Interaction of HSD1 and AA with the Compounds

Target	Compounds	Binding Affinity (kcal/mol)	Inhibition Constant (µM)
AA	Stigmasterol	−9.6	1.27×10^{-1}
	4,4-Dimethylcyclohex-2-en-1-ol	−7.4	3.71
	Palmitic acid	−5.8	55.44
	Oleic Acid	−5.7	65.65
	Metformin	−5.2	152.81
HSD1	Stigmasterol	−9.4	1.27×10^{-1}
	4,4-Dimethylcyclohex-2-en-1-ol	−7.2	5.21
	Pyrogallol	−5.7	65.65
	7,11-Hexadecadien-1-ol, acetate, (7Z,11Z)-	−5.7	65.65
	Metformin	−5.6	77.73

Figure 5 depicts the dock pose and docking interactions of stigmasterol and metformin with AA and HSD1.
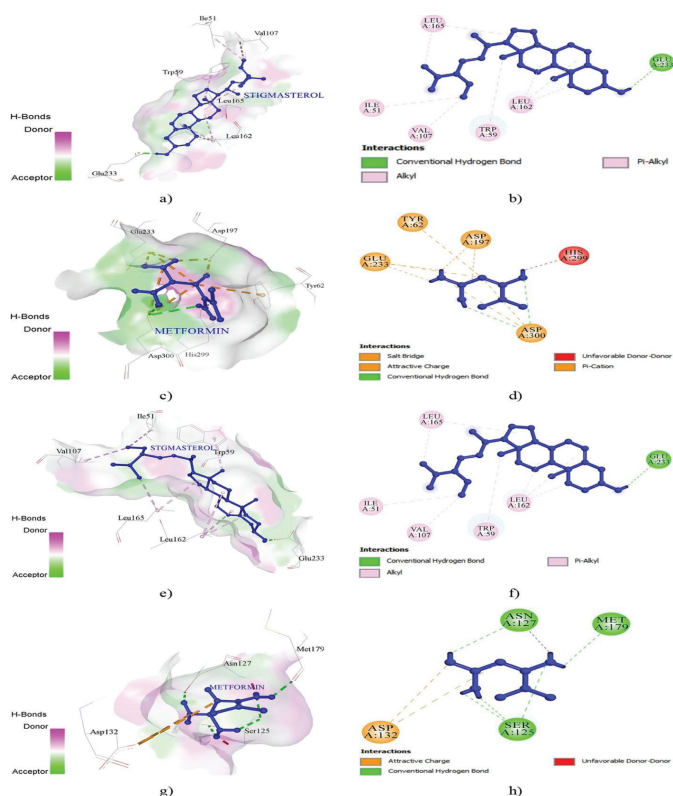

Figure 5. The respective 3D and 2D dock pose of stigmasterol and metformin with AA; stigmasterol (a and b) and aspirin (c and d), HSD1; stigmasterol (e and f) and metformin (g and h)

The MDS result of the stigmasterol docked AA is presented in Figure 6 showing the cluster (a) and residue (b) fluctuations. Notable higher fluctuations for stigmasterol were observed at Val129 (2.29 Å), Gly144 (3.11 Å), Glu240 (3.01 Å), Gly306 (3.22 Å), and Ser482 (3.21 Å) with the highest at Gly351 (5.80 Å). Higher fluctuations for metformin were observed at Gln7 (2.67 Å), Pro54 (2.45 Å), Asp138 (3.52 Å), Leu217 (3.78 Å), Asp375 (3.30 Å), and Gly460 (3.12 Å). AA emerged as a therapeutic antidiabetic target for hyperglycemic control due to its involvement in the digestion of polysaccharides to mono and disaccharides leading to postprandial hyperglycemia (Kaur et al., 2021). The result of the present study showed potential AA inhibition by stigmasterol depicted by the stable interaction with low BA and Ki. Additionally, structural deformability was observed within the peptide structure demonstrating flexibility and hinge regions within the structure.

Figure 6 presents the MDS result HSD1 docked with stigmasterol exhibiting cluster (c) and residue (d) fluctuations. A major residue and cluster fluctuation was observed at the C-terminal with the highest seen at Tyr284 (5.76 Å). However, notable higher fluctuations for stigmasterol were seen at Gln33 (2.23), Leu128 (2.73), Val206 (2.46 Å), Val227 (2.58 Å), and Pro271 (2.05). For metformin, the highest fluctuation was observed at the

N-terminal at Pro29 (3.10) and Pro178 (1.88). Therefore, stigmasterol demonstrated higher fluctuation than metformin. The physiological involvement of HSD1 in the conversion of cortisone to active cortisol contributes to insulin resistance, hyperglycemia, and other metabolic modifications. Thus, an attractive antidiabetic target (Almeida et al., 2021). In this report, stigmasterol showed promising inhibitory potential against this enzyme evident in its low BA and Ki interactions. MDS of the enzymes also showed possible deformability and flexibility with the enzyme structure, further supporting the inhibitory potential of stigmasterol.
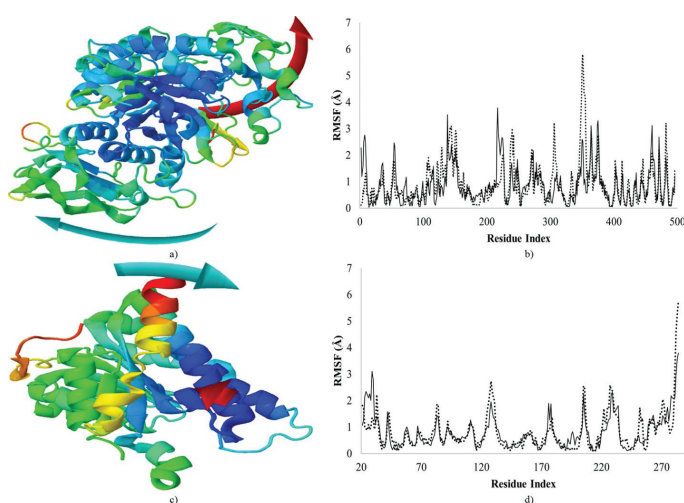

Figure 4. MDS result of stigmasterol and metformin showing respective cluster movement and residue fluctuations of the docked complexes; AA (a and b) and HSD1 (c and d)

4.   Conclusion

In the present study, the researchers explored the antioxidant, anti-inflammatory, and antidiabetic potential of XA in silico. Persistent hyperglycemia, OS, and inflammation are key contributors to the development of diabetes and stigmasterol showed good inhibitory potential against the proteins involved in OS and inflammation processes though 4,4-Dimethylcyclohex-2-en-1-ol also demonstrated its potential inhibitory candidacy. Additionally, both compounds exhibited possible antihyperglycemic potential against hyperglycemic targets. However, a confirmative mechanistic inhibitory study of these compounds against the targets in the present study are required to ascertain their inhibitory effects. Conclusively, stigmasterol and 4,4-Dimethylcyclohex-2-en-1-ol might be the key compounds involved in the antioxidant, anti-inflammatory, and antidiabetic activity of XA *via* inhibition of the enzymes involved in OS, inflammation, and diabetes.

References

1.   Almeida C, Monteiro C, Silvestre S. Inhibitors of 11β-hydroxysteroid dehydrogenase type 1 as potential drugs for type 2 diabetes mellitus—a systematic review of clinical and in vivo preclinical studies. Vol. 89, Scientia Pharmaceutica. 2021.

2.   Bakrim W Ben, Nurcahyanti ADR, Dmirieh M, Mahdi I, Elgamal AM, El Raey MA, et al. Phytochemical Profiling of the Leaf Extract of Ximenia americana var. caffra and Its Antioxidant, Antibacterial, and Antiaging Activities in Vitro and in Caenorhabditis elegans: A Cosmeceutical and Dermatological Approach. Oxid Med Cell Longev. 2022;2022.

3.   Bhatti JS, Sehrawat A, Mishra J, Sidhu IS, Navik U, Khullar N, et al. Oxidative stress in the pathophysiology of type 2 diabetes and related complications: Current therapeutics strategies and future perspectives. Free Radic Biol Med. 2022 May;184:114–34.

4.   Chalimoniuk M. [Secretory phospholipase A2 and its role in oxidative stress and inflammation]. Vol. 58, Postepy biochemii. 2012.

5.   Chen S, Chen H, Du Q, Shen J. Targeting Myeloperoxidase (MPO) Mediated Oxidative Stress and Inflammation for Reducing Brain Ischemia Injury: Potential Application of Natural Compounds. Vol. 11, Frontiers in Physiology. 2020.

6.   da Silva-Leite KES, Girão DKFB, de Freitas Pires A, Assreuy AMS, de Moraes PAF, Cunha AP, et al. Ximenia americana heteropolysaccharides ameliorate inflammation and visceral hypernociception in murine caerulein-induced acute pancreatitis: Involvement of CB2 receptors. Biomedicine & Pharmacotherapy. 2018 Oct;106:1317–24.

7.   da Silva BAF, Pessoa RT, da Costa RHS, de Oliveira MRC, Ramos AGB, de Lima Silva MG, et al. Evaluation of the antiedematogenic and anti-inflammatory properties of Ximenia americana L. (Olacaceae) bark extract in experimental models of inflammation. Biomedicine & Pharmacotherapy. 2023 Oct;166:115249.

8.   Dahiru MM. Recent advances in the therapeutic

potential phytochemicals in managing diabetes. Journal of Clinical and Basic Research. 2023;7(1):13–20.

9. Mubarak Muhammad Dahiru, Enoch Buba Badgal, Neksumi Musa. Phytochemistry, GS-MS analysis, and heavy metals composition of aqueous and ethanol stem bark extracts of Ximenia americana. GSC Biological and Pharmaceutical Sciences. 2022;21(3).

10. Dahiru MM, MN, AAM, & AMA. Potential Antidiabetic Compounds from Anogeissus leiocarpus: Molecular Docking, Molecular Dynamic Simulation, and ADMET Studies. Borneo Journal of Pharmacy. 2023;6(3).

11. Dahiru M, Samuel N. A review of the mechanisms of action and side effects of anti-diabetic agents. Trends in Pharmaceutical Sciences [Internet]. 2022 Sep [cited 2024 Mar 4];8(3). Available from: https://doi.org/10.30476/tips.2022.95931.1153

12. De Nardo D, Balka KR, Cardona Gloria Y, Rao VR, Latz E, Masters SL. Interleukin-1 receptor–associated kinase 4 (IRAK4) plays a dual role in myddosome formation and Toll-like receptor signaling. Journal of Biological Chemistry. 2018 Sep;293(39):15195–207.

13. Ellulu MS, Samouda H. Clinical and biological risk factors associated with inflammation in patients with type 2 diabetes mellitus. BMC Endocr Disord. 2022 Jan 6;22(1):16.

14. Ferenczy GG, Kellermayer M. Contribution of hydrophobic interactions to protein mechanical stability. Comput Struct Biotechnol J. 2022;20.

15. Gandhi Y, Kumar R, Grewal J, Rawat H, Mishra SK, Kumar V, et al. Advances in anti-inflammatory medicinal plants and phytochemicals in the management of arthritis: A comprehensive review. Food Chemistry Advances. 2022 Oct;1:100085.

16. Jendele L, Krivak R, Skoda P, Novotny M, Hoksza D. PrankWeb: a web server for ligand binding site prediction and visualization. Nucleic Acids Res. 2019 Jul 2;47(W1):W345–9.

17. Kaur N, Kumar V, Nayak SK, Wadhwa P, Kaur P, Sahu SK. Alpha-amylase as molecular target for treatment of diabetes mellitus: A comprehensive review. Chem Biol Drug Des. 2021 Oct 4;98(4):539–60.

18. Kefelegn GA, Desta B. Ximenia americana: Economic Importance, Medicinal Value, and Current Status in Ethiopia. The Scientific World Journal. 2021 Mar 8;2021:1–7.

19. Korac B, Kalezic A, Pekovic-Vaughan V, Korac A, Jankovic A. Redox changes in obesity, metabolic syndrome, and diabetes. Redox Biol. 2021;42.

20. Kurcinski M, Oleniecki T, Ciemny MP, Kuriata A, Kolinski A, Kmiecik S. CABS-flex standalone: A simulation environment for fast modeling of protein flexibility. Bioinformatics. 2019;35(4).

21. López-Blanco JR, Aliaga JI, Quintana-Ortí ES, Chacón P. IMODS: Internal coordinates normal mode analysis server. Nucleic Acids Res. 2014;42(W1).

22. Nwozo OS, Effiong EM, Aja PM, Awuchi CG. Antioxidant, phytochemical, and therapeutic properties of medicinal plants: a review. Int J Food Prop. 2023 Sep 22;26(1):359–88.

23. Oguntibeju OO. Type 2 diabetes mellitus, oxidative stress and inflammation: examining the links. Int J Physiol Pathophysiol Pharmacol. 2019;11(3).

24. Ortiz CLD, Completo GC, Nacario RC, Nellas RB. Potential Inhibitors of Galactofuranosyltransferase 2 (GlfT2): Molecular Docking, 3D-QSAR, and In Silico ADMETox Studies. Sci Rep. 2019 Nov 19;9(1):17096.

25. Pallan PS, Wang C, Lei L, Yoshimoto FK, Auchus RJ, Waterman MR, et al. Human cytochrome P450 21A2, the major steroid 21-hydroxylase: Structure of the enzyme•progesterone substrate complex and rate-limiting C–H bond cleavage. Journal of Biological Chemistry. 2015;290(21).

26. Papi S, Ahmadizar F, Hasanvand A. The role of nitric oxide in inflammation and oxidative stress. Immunopathologia Persa. 2019 Apr 13;5(1):e08–e08.

27. Przeor M. Some Common Medicinal Plants with Antidiabetic Activity, Known and Available in Europe (A Mini-Review). Vol. 15, Pharmaceuticals. 2022.

28. Sangwung P, Petersen KF, Shulman GI, Knowles JW. Mitochondrial Dysfunction, Insulin Resistance, and Potential Genetic Implications. Endocrinology. 2020 Apr 1;161(4).

29. Sanner MF. Python: A programming language for software integration and development. Vol. 17, Journal of Molecular Graphics and Modelling. 1999.

30. Shettar AK, Kotresha K, Kaliwal BB, Vedamurthy AB. Evaluation of in vitro antioxidant and anti-inflammatory activities of Ximenia americana extracts. Asian Pac J Trop Dis. 2015 Nov;5(11):918–23.

31. Shettar AK, Sateesh MK, Kaliwal BB, Vedamurthy AB. In vitro antidiabetic activities and GC-MS phytochemical analysis of Ximenia americana extracts. South African Journal of Botany. 2017 Jul;111:202–11.

32. Shields HJ, Traa A, Van Raamsdonk JM. Beneficial and Detrimental Effects of Reactive Oxygen

Species on Lifespan: A Comprehensive Review of Comparative and Experimental Studies. Vol. 9, Frontiers in Cell and Developmental Biology. 2021.

33. Singh A, Singh K, Sharma A, Kaur K, Chadha R, Singh Bedi PM. Past, present and future of xanthine oxidase inhibitors: design strategies, structural and pharmacological insights, patents and clinical trials. RSC Med Chem. 2023;14(11):2155–91.

34. Veith A, Moorthy B. Role of cytochrome P450s In the generation and metabolism of reactive oxygen species. Vol. 7, Current Opinion in Toxicology. 2018.

35. Wronka M, Krzemińska J, Młynarska E, Rysz J, Franczyk B. The Influence of Lifestyle and Treatment on Oxidative Stress and Inflammation in Diabetes. Vol. 23, International Journal of Molecular Sciences. 2022.

36. Yoshimoto FK, Zhou Y, Peng HM, Stidd D, Yoshimoto JA, Sharma KK, et al. Minor activities and transition state properties of the human steroid hydroxylases cytochromes P450c17 and P450c21, from reactions observed with deuterium-labeled substrates. Biochemistry. 2012;51(36).

37. Yousef H, Khandoker AH, Feng SF, Helf C, Jelinek HF. Inflammation, oxidative stress and mitochondrial dysfunction in the progression of type II diabetes mellitus with coexisting hypertension. Front Endocrinol (Lausanne). 2023;14.

38. Zhang P, Li T, Wu X, Nice EC, Huang C, Zhang Y. Oxidative stress and diabetes: antioxidative strategies. Vol. 14, Frontiers of Medicine. 2020.